Partial anhysteretic remanent magnetization in magnetite 1. Additivity

Yongjae Yu, David J. Dunlop, and Özden Özdemir

Geophysics, Department of Physics, University of Toronto, Toronto, Ontario, Canada

Received 15 February 2001; revised 8 February 2002; accepted 13 February 2002; published 23 October 2002.

[1] We have tested the additivity of partial anhysteretic remanent magnetization (pARM) for suites of eight synthetic magnetites with mean grain sizes from 65 nm to 18 μm and 18 natural samples including lake sediments, oceanic and continental volcanic rocks, gabbros, and granites. In both synthetic and natural sample suites, domain states inferred from hysteresis and other magnetic properties vary from single-domain (SD) through pseudosingle-domain (PSD) to multidomain (MD). For each sample, total ARM intensity was compared with sums of partial ARMs of three different types: four conjugate pairs of parallel pARMs; four pairs of perpendicular pARMs; and one set of five neighboring parallel pARMs. In each case, the intervals of alternating field (AF) over which a steady field H was applied to produce the partial ARMs are nonoverlapping and cover the entire AF range (0–100 mT) used to produce the total ARM. Additivity of partial ARMs was verified to better than ±3% for all the samples, whatever the domain state (SD, PSD, and MD) or composition (ranging from pure magnetite to $x = 0.6$ titanomagnetite). The universality of pARM additivity is unexpected because its analog, partial thermoremanent magnetization (pTRM), deviates from ideal behavior as the grain size increases and the domain structure becomes MD. The different behaviors probably result from the fact that pARM is produced at ordinary temperatures over short times, whereas the most intense pTRM is produced at temperatures approaching the Curie point with significant dwell times, promoting such processes as isothermal remanence acquisition, domain nucleation, and domain wall reequilibration. Verification of the law of additivity of pARMs is an encouraging first step toward validating pseudo-Thellier and other methods of paleointensity determination that use ARM in place of, or in addition to, TRM. *INDEX TERMS:* 1521 Geomagnetism and Paleomagnetism: Paleointensity; 1540 Geomagnetism and Paleomagnetism: Rock and mineral magnetism; 1518 Geomagnetism and Paleomagnetism: Magnetic fabrics and anisotropy; 1594 Geomagnetism and Paleomagnetism: Instruments and techniques; *KEYWORDS:* additivity, magnetite, ARM, pseudo-Thellier, AF demagnetization

Citation: Yu, Y., D. J. Dunlop, and Ö. Özdemir, Partial anhysteretic remanent magnetization in magnetite, 1, Additivity, *J. Geophys. Res.*, *107*(B10), 2244, doi:10.1029/2001JB001249, 2002.

1. Introduction

[2] Anhysteretic remanent magnetization (ARM) is produced by the combination of a slowly decaying alternating field (AF) $\tilde{H}$ and a steady unidirectional field H. ARM is important because of its analogy to thermoremanent magnetization (TRM), as first proposed by *Rimbert* [1959]. ARM has been widely used as a normalizing remanence in relative geomagnetic field intensity determination on sediments [*Tauxe*, 1993], on the implicit assumption that ARM is also an analog of depositional remanence (DRM). Techniques involving ARM have sometimes been used to determine absolute paleointensities, as discussed below. However, compared to TRM and partial TRM (pTRM), the fundamental properties of ARM and partial ARM (pARM) are still poorly known [*Rimbert*, 1959; *Patton and Fitch*, 1962; *Dunlop and West*, 1969; *Levi and Merrill*, 1976; *Dunlop*, 1981; *Jackson et al.*, 1988; *Dunlop and Özdemir*, 1997].

[3] To avoid mineralogical alteration caused by repeated heatings in the classic Thellier method of paleointensity determination [*Thellier and Thellier*, 1959], analog methods that substitute ARM for TRM have been proposed. ARM techniques compare AF coercivity spectra instead of comparing unblocking temperature spectra as in Thellier-type methods. Paleointensity determinations based on the ratio R of TRM/ARM intensities have been reported by *Markert and Heller* [1972], *Banerjee and Mellema* [1974], *Stephenson and Collinson* [1974], and *Bagina and Petrova* [1977]. However, experimentally determined R values are inconsistent, the uncertainty being often as large as an order of magnitude [*Bailey and Dunlop*, 1977]. A better method that compares intensities and coercivity spectra of ARM produced before and after heating, proposed by *Shaw* [1974],

0148-0227/02/2001JB001249$09.00

Table 1. Grain Size Determinations for Synthetic Powders[a]

Powder	Counts	$m \pm \sigma_m$, μm	$n \pm \sigma_n$, μm	$q \pm \sigma_q$	$d \pm \sigma_d$, μm	Previous d, μm
4000	884	0.068 ± 0.037	0.049 ± 0.029	1.48 ± 0.42	0.065 ± 0.036	0.025[b]
5099	1300	0.22 ± 0.11	0.16 ± 0.08	1.44 ± 0.42	0.21 ± 0.10	0.12[b]
112978	1022	0.44 ± 0.2	0.34 ± 0.16	1.33 ± 0.29	0.44 ± 0.20	0.19[b]
M	532	0.24 ± 0.07	0.19 ± 0.06	1.29 ± 0.28	0.24 ± 0.07	0.2[c]
5000	1262	0.38 ±0.24	0.25 ± 0.17	1.65 ± 0.63	0.34 ± 0.21	0.75[d]
3006	1471	1.18 ± 0.81	0.77 ± 0.53	1.62 ± 0.54	1.06 ± 0.71	1[b]
112982	1618	18.6 ± 9.6	12.3 ± 6.4	1.61 ± 0.58	16.9 ± 8.3	37.5[d]
041183	870	20.1 ± 13.4	13.4 ± 9.1	1.57 ± 0.54	18.3 ± 12.0	40[d]

[a] Powders 4000, 112978, 5000, 3006, 112982, and 041183 are from the Wright Company; powders 5099 and M are the products of Pfizer and Mapico Companies; m and n are major and minor axes of the rectangular grains; q is the axial ratio; d is the estimated mean grain size; uncertainty corresponds to one standard deviation.
[b] *Özdemir and Banerjee* [1982].
[c] *Levi and Merrill* [1978].
[d] *Jackson et al.* [1990].

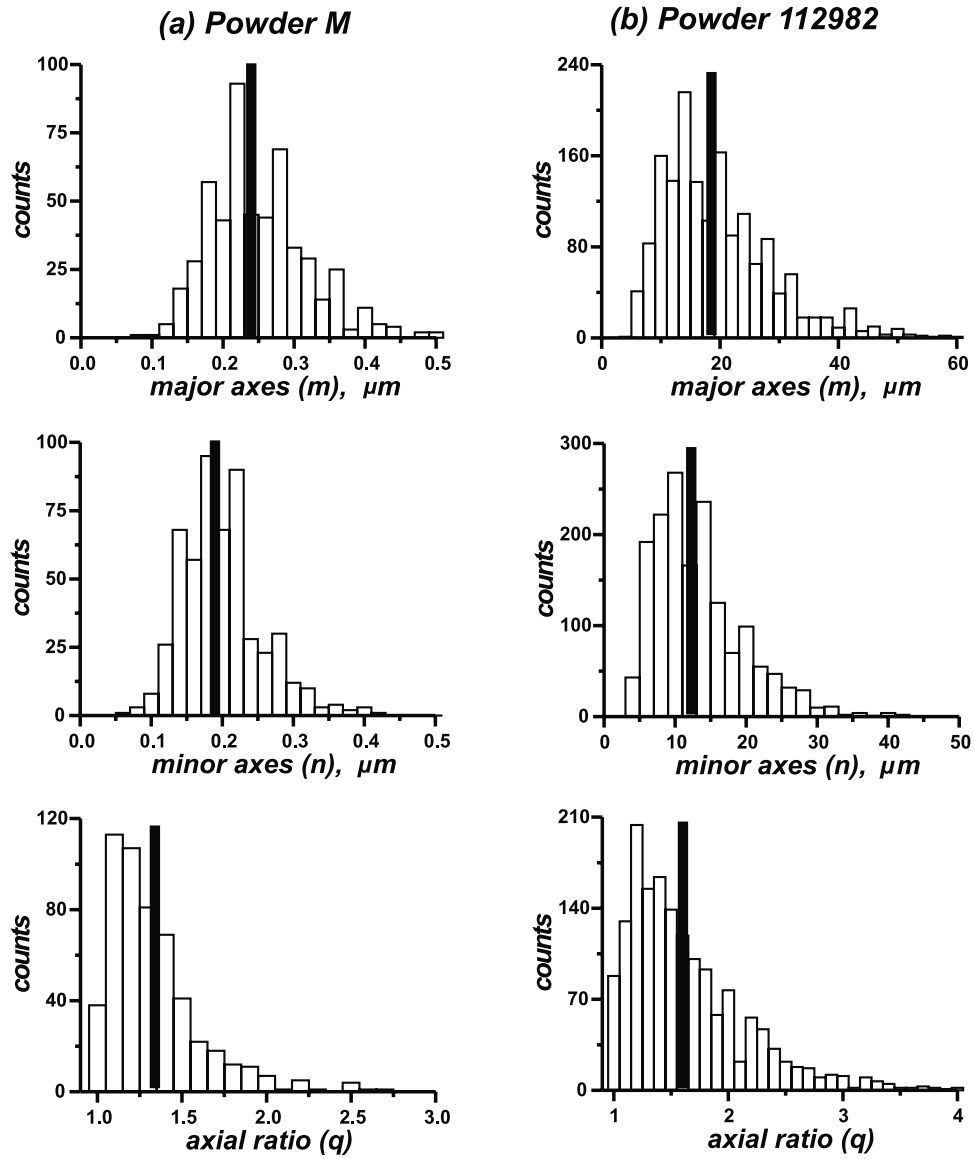

Figure 1. Distributions of major and minor axes, m and n, and axial ratio q determined from grain counts in SEM photos for (a) powder M and (b) powder 112982 (five grains with $m > 60$ μm and seven grains with $q > 4$ fall beyond the region plotted).

Table 2. Synthetic Samples[a]

		Physical Properties			Magnetic Properties	Hysteresis Properties				
Sample	Powder	d, μm	f, %	matrix	MDF, mT	n	M_s, μA m^2	M_{rs}, μA m^2	H_c, mT	H_{cr}, mT
1	4000	0.065	0.5	CaF_2	30	6	415.2	168.7	24.88	33.95
2	5099	0.21	0.5	CaF_2	24	6	220.8	49.7	18.73	36.85
3	112978	0.44	0.5	CaF_2	30	6	526.7	62.3	11.10	32.40
4	M	0.24	0.5	CaF_2	28	6	350.0	129.3	33.07	64.17
5	5000	0.34	0.5	CaF_2	34	6	542.2	194.6	32.63	51.15
6	3006	1.06	0.5	CaF_2	33	6	1926.8	560.8	23.67	42.02
7	112982	16.9	0.5	CaF_2	10	6	1184.0	67.3	5.02	32.47
9			1.0	Kaolin	10					
8	041183	18.3	0.5	CaF_2	10	6	897.5	58.6	6.06	31.13
10			1.0	Kaolin	10					

[a] Here d is the mean grain size; f is the magnetite concentration; MDF is the median destructive field (MDF) determined from AF demagnetization of ARM; n is the number of measured subsamples; values of saturation magnetization (M_s), saturation remanence (M_{rs}), and coercive force (H_c) were determined from hysteresis loops; values of remanence coercivity (H_{cr}) were obtained from backfield measurements; σ is the standard deviation.

has been refined by *Kono* [1978], *Senanayake et al.* [1982], *Rolph and Shaw* [1985] and *Tsunakawa and Shaw* [1994]. Recently, *Valet and Herrero-Bervera* [2000] reassessed the Van Zijl method [*Van Zijl et al.*, 1962], comparing AF demagnetization spectra of natural remanent magnetization (NRM) and TRM, but its general applicability in absolute paleointensity determination remains to be shown. To extract relative paleointensity information from sedimentary sequences, a pseudo-Thellier method that avoids heating, and thus chemical alteration, was developed by *Tauxe et al.* [1995]. The pseudo-Thellier method compares increments of NRM destroyed in a series of AF demagnetization steps with increments of pARM acquired in a laboratory field in matching AF steps. (Note that the NRM in sediments was acquired in a post-depositional magnetization process, not as TRM; hence only relative paleointensity can be found.) The pseudo-Thellier method compares pARM gained with NRM lost in companion AF steps. It is thus in the spirit of the *Coe* [1967] version of the Thellier method, which compares pTRM gained and NRM lost in pairs of heatings. Other methods involving ARM compare destructive AF spectra of total ARM and NRM: the incremental comparison of pARM acquisition and NRM loss in companion steps is lacking.

[4] Thellier-type paleointensity determinations are considered the most reliable because additivity, reciprocity, and independence of pTRMs have been experimentally demonstrated for single-domain (SD) grains [*Thellier*, 1938]. In order to provide a similar rationale for the pseudo-Thellier method, pARMs must be shown to obey laws analogous to the Thellier laws for pTRMs:

1. The law of additivity: Partial ARMs must be additive, pARM ($\widetilde{H}_2$, $\widetilde{H}_1$) + pARM ($\widetilde{H}_3$, $\widetilde{H}_2$) + pARM ($\widetilde{H}_i$, $\widetilde{H}_{i-1}$) = pARM ($\widetilde{H}_i$, $\widetilde{H}_1$),where the are $\widetilde{H}_i$ AFs.

2. The law of reciprocity: pARM ($\widetilde{H}_2$, $\widetilde{H}_1$) must be AF demagnetized over precisely the interval ($\widetilde{H}_2$, $\widetilde{H}_1$).

3. The law of independence: pARM ($\widetilde{H}_2$, $\widetilde{H}_1$), acquired with a steady field applied over the AF interval ($\widetilde{H}_2$, $\widetilde{H}_1$), must be independent of pARMs produced over field intervals that do not overlap ($\widetilde{H}_2$, $\widetilde{H}_1$).

[5] The purpose of this paper and the companion paper by *Yu et al.* [2002] (hereinafter referred to as paper 2) is to investigate systematically the additivity and reciprocity of pARMs. Experimental tests of the independence of pARMs will be reported elsewhere.

2. Samples

2.1. Synthetic Samples

[6] Eight commercial magnetite powders, with domain states and mean grain sizes ranging from SD (0.065 μm) to multidomain (MD) (18.3 μm), were studied (Table 1). Grain sizes were determined using a Hitachi S-4500 scanning electron microscope (SEM). The grains are predominantly rectangular in cross section. From the measured major axis m and minor axis n of each grain, the equivalent circular diameter $d = 2\ (m \cdot n/\pi)^{1/2}$ and the axial ratio $q = m/n$ were calculated.

[7] Experimental averages of m, n, q, and d are summarized in Table 1. Except for powder M (Mapico), the grain size distributions are broad and skewed toward small sizes, resembling Poisson or lognormal distributions (Figure 1). To reduce the uncertainty, ≥1000 grains were typically

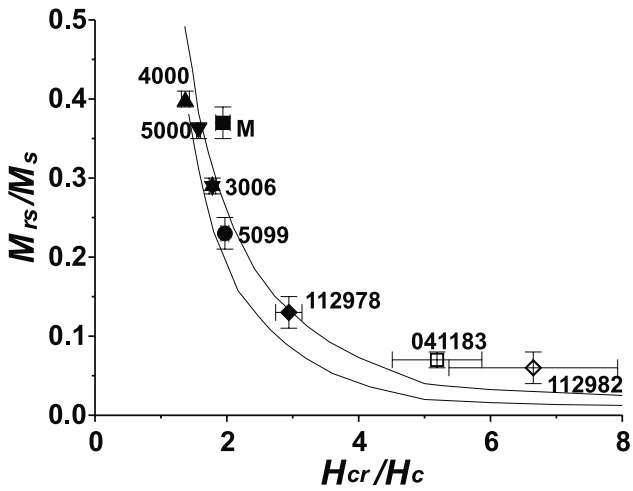

Figure 2. A Day plot of hysteresis data for the synthetic powders. Solid lines are proposed mixing curves as by *Dunlop* [2002].

Table 3. Natural Samples[a]

Sample			Magnetic Properties		Hysteresis Properties				
Label	Lithology	Ref.	MDF, mT	T_{UB}, °C	n	M_s, μA m^2	M_s, μA m^2	H_c, mT	H_{cr}, mT
An 1	andesite	1	29	580	6	429.8	131.1	20.88	39.18
An 3	andesite	1	30	580	6	868.5	203.2	14.73	34.28
C 6	gabbro	2	39	580	6	990.0	274.2	19.63	40.80
C 12	gabbro	2	40	580	8	50.4	17.7	28.10	43.46
T 2	gabbro	3	37	580	6	772.3	284.5	26.35	42.58
T 19	gabbro	3	37	580	6	853.0	253.8	22.52	40.03
Bu 5	granite	4	13	580	6	371.0	18.4	9.98	40.77
Bu 8	granite	4	18	580	6	1083.4	28.2	7.44	39.82
S 50	granite	5	13	580	6	1120.4	48.7	9.11	39.98
456A	lake sediment	6	31	580[b]	8	93.7	18.8	16.11	36.84
456B	lake sediment	6	31						
578A	lake sediment	6	33	580[b]	6	102.4	26.2	20.88	39.37
578B	lake sediment	6	33						
P 6	oceanic basalt	7,8	24	160[c]	na	na		na	
P 7	oceanic basalt	7,8	25	∼	na	na		na	
P 8	oceanic basalt	7,8	41	260[c]	na	na		na	
Na 2	pumice	1	24	580	6	88.3	25.8	21.22	36.70
Km 3	red scoria	1	48	500	6	1146.8	445.8	37.47	61.90

[a] MDF is the median destructive field (MDF) determined from AF demagnetization of ARM; T_{UB} is the maximum unblocking temperature from the thermal demagnetization of sister specimens; n is the number of measured chips; na is not available; references are 1, *Yu* [1998]; 2, *Yu and Dunlop* [2001]; 3, *Yu and Dunlop* [2002]; 4, *Dunlop* [1984]; 5, *Dunlop et al.* [1984]; 6, *Brachfeld and Banerjee* [2000]; 7, *Batiza et al.* [1996]; and 8, *Gee and Kent* [1999].

[b] Curie point from high-field thermomagnetic curves (S. Brachfeld, personnel communication).

[c] Curie point from the temperature dependence of weak-field susceptibility (J. Gee, personnel communication).

measured from at least six SEM photos per powder. Our estimated mean diameters are different in some cases from those advertised or previously reported [*Levi and Merrill*, 1978; *Özdemir and Banerjee*, 1982; *Jackson et al.*, 1990].

[8] Ten samples were prepared using the magnetic powders (Table 2). Samples 1–8 are ≈0.5% by volume dispersions of magnetite in a matrix of CaF_2 (mean grain size 10 μm). Cylindrical pellets 8.8 mm in diameter and 8.6 mm in height were pressed and then tightly wrapped with quartz wool inside quartz capsules. The capsules were sealed under vacuum and annealed for 3 hours at 700°C to stabilize the magnetic properties [*Levi and Merrill*, 1978; *Dunlop and Argyle*, 1997].

[9] Samples 9 and 10 are ≈1.0% by volume dispersions of powder 112982 and 041183 in a matrix of kaolin, intended to study the possible effect of varying magnetite concentration (Table 2). These two samples, 23 mm in diameter and 21 mm in height, were not vacuum sealed nor annealed because kaolin produces water during heating.

[10] Room temperature hysteresis measurements were performed on six samples of each powder using an alternating gradient force magnetometer. The hysteresis parameters saturation remanence M_{rs}, saturation magnetization M_s, and coercive force H_c were calculated after high-field slope correction. Remanent coercive force H_{cr} was obtained from backfield measurements.

[11] Averages of the six measurements of M_{rs}/M_s and H_{cr}/H_c for each powder appear in Table 2. The same M_{rs}/M_s and H_{cr}/H_c data are plotted in Figure 2 (a Day plot [*Day et al.*, 1977]). Powders 4000, 5000, and M have the most SD-like characteristics: M_{rs}/M_s = 0.36–0.4 and H_{cr}/H_c < 2. Powders 3006, 5099, and 112978 lie along a typical pseudosingle-domain (PSD) trend [*Dunlop*, 2002]. Low values of M_{rs}/M_s (<0.1) and high values of H_{cr}/H_c (>5) characterize MD powders 041183 and 112982. Interestingly, powder 5099 shows more PSD-like behavior than M or 5000 despite its smaller grain size (Figure 2 and Table 2).

2.2. Natural Samples

[12] Eighteen natural samples were also studied: two andesites, four gabbros, three granites, four lake sediments, three oceanic basalts, one pumice, and one red scoria (Table 3). The rocks selected have magnetic and paleomagnetic properties that are well documented. They were chosen from a large collection of several hundred cores on the basis of their low magnetic fabric anisotropy (see sample selection criteria in

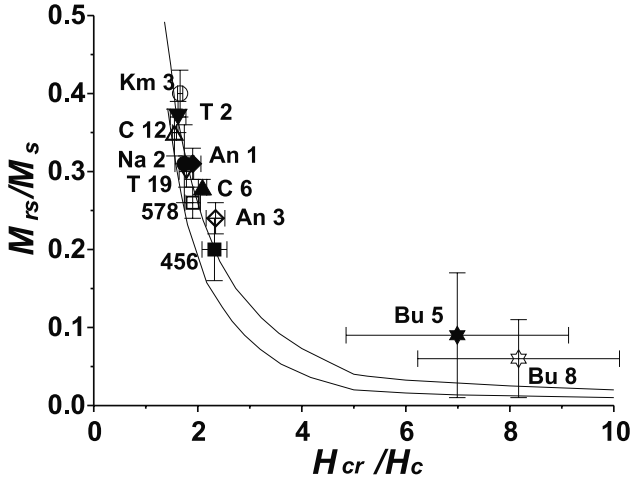

Figure 3. A Day plot of hysteresis ratios for the natural rocks. BU 5 and 8 (and S 50, which falls to the right of the region plotted) have MD character. Solid lines are proposed mixing curves as by *Dunlop* [2002].

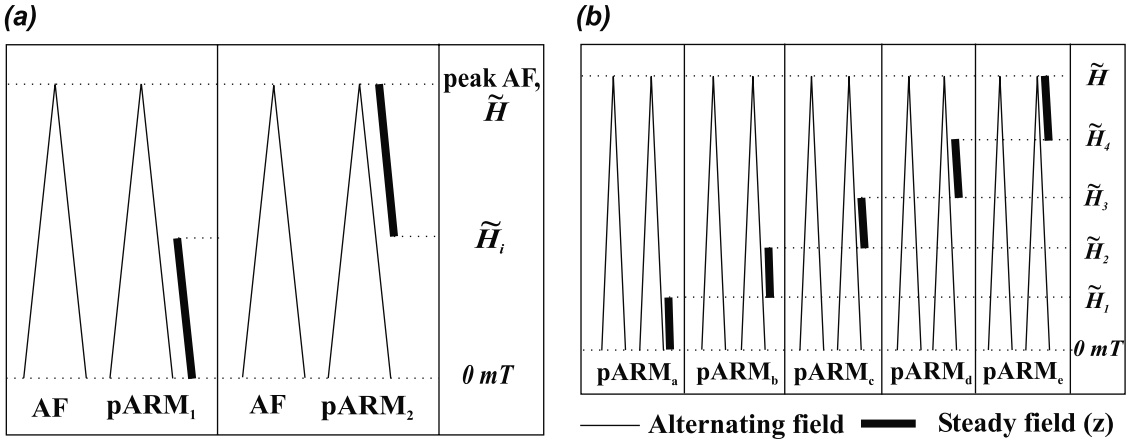

Figure 4. Schematic diagrams of pARM acquisition. (a) Conjugate pairs pARM$_1$ ($\widetilde{H}$, 0 mT) and pARM$_2$ (100 mT, $\widetilde{H}$) were produced starting from a peak AF of 100 mT, with an added steady field H on from $\widetilde{H}$ to 0 mT and on from 100 mT to $\widetilde{H}$, respectively. (b) The five neighboring pARMs, pARM$_a$, pARM$_b$; pARM$_e$ were produced with H added during adjacent AF intervals, as shown.

section 3.1). Most samples are cylindrical, 2.3 cm in diameter and 2.0 cm in height, but the oceanic basalts are 1.2-cm cubes.

[13] The An-ei Andesites (An 1, 3) and Nabeyama Pumice (Na 2) are from Mount Sakurajima, Japan [*Yu*, 1998]. The Kometsuka red scoria (Km 3) from Mount Aso, Japan has the most SD-like behavior, with the largest median destructive field (MDF) during AF demagnetization of ARM, the highest M_{rs}/M_s value and the lowest H_{cr}/H_c value (Table 3). The Cordova Gabbro (C6, 12) and Tudor Gabbro (T2, 19) samples were included because of their successful Thellier paleointensity determinations [*Yu and Dunlop*, 2001, also manuscript in preparation, 2002]. The lake sediment samples (456A, B; 578A, B) are from Lake Pepin, Minnesota [*Brachfeld and Banerjee*, 2000] and the three oceanic basalts (P6–8) are from the East Pacific Rise [*Batiza et al.*, 1996; *Gee and Kent*, 1999]. In order to study ARM properties of MD magnetite-bearing rocks, two granites (BU 5, 8) from Burchell Lake, Ontario [*Dunlop*, 1984] and one granite (S 50) from Shelley Lake, Ontario [*Dunlop et al.*, 1984] were used.

[14] In the Day plot, the values of M_{rs}/M_s and H_{cr}/H_c of chips from most rocks form tight clusters in the SD to small PSD range (Figure 3). Hysteresis ratios of the granites scatter more broadly in the MD region, perhaps reflecting a wide grain size distribution of magnetite in granite samples.

3. Experimental Procedures

3.1. Sample Selection Criteria

[15] The first requirement is a reproducible stable ARM. Samples were initially demagnetized in a peak AF of 100 mT using a Molspin demagnetizer. ARM was then produced in a 100-mT AF with an added steady field (usually 50 μT) applied along the specimen axis. AF demagnetization and ARM acquisition were repeated six or more times over a period of six weeks to detect possible intensity variations. Both AF-demagnetized remanences and ARMs were required to be reproducible within 3%.

[16] A second requirement, which is less easily satisfied than the first, is sample isotropy. This criterion was intended

Table 4. Experimental Results for Additivity of Pairs of Parallel pARMs for Synthetic Samples[a]

Sample	$\widetilde{H}_i$, mT	pARM$_1$, mA/m	pARM$_2$, mA/m	$\sum$ pARM, mA/m	ARM, mA/m
1	20	3.46	16.28	19.74	19.68
	30	7.76	11.84	19.61	
	40	12.49	7.29	19.66	
	50	15.12	4.50	19.59	
2	20	3.63	17.22	20.85	20.88
	30	8.86	12.02	20.88	
	40	14.09	6.80	20.88	
	50	17.25	3.45	20.70	
3	20	4.63	22.85	27.47	27.53
	30	10.4	17.35	27.74	
	40	15.88	11.91	27.79	
	50	20.43	7.22	27.65	
4	20	6.95	27.86	34.81	35.26
	30	16.25	18.73	34.98	
	40	23.7	11.64	35.34	
	50	28.74	6.42	35.16	
5	20	1.74	8.57	10.31	10.30
	30	3.71	6.39	10.10	
	40	5.53	4.85	10.37	
	50	7.27	3.24	10.51	
6	20	2.98	13.12	16.10	16.05
	30	5.82	10.27	16.09	
	40	8.90	6.98	15.89	
	50	12.01	4.32	16.34	
7	5	1.13	7.19	8.27	8.27
	10	2.97	5.07	8.03	
	20	5.17	3.09	8.25	
	30	6.58	1.57	8.15	
8	5	0.92	7.44	8.35	8.27
	10	2.40	5.75	8.15	
	20	4.92	3.23	8.15	
	30	6.32	1.92	8.23	
9	5	8.26	81.30	89.48	89.11
	10	25.67	63.37	89.00	
	20	50.02	39.21	89.18	
	30	63.58	25.70	89.26	
10	5	18.93	119.04	137.94	137.79
	10	49.90	86.77	136.59	
	20	80.79	56.58	137.37	
	30	100.19	37.37	137.54	

[a] During pARM acquisition, the steady field of 50 μT was on from 100 mT to for pARM$_2$ and on from $\widetilde{H}$ to 0 mT for pARM$_1$. Σ pARM is the sum pARM$_1$ + pARM$_2$.

Table 5. Experimental Results for Additivity of Pairs of Parallel pARMs for Natural Samples

Sample	H, μT	$\widetilde{H}$, mT	$pARM_1$, mA/m	$pARM_2$, mA/m	$\sum$ pARM, mA/m	ARM, mA/m
An 1	50	20	542.9	1424.4	1967.2	1960.1
		30	826.5	1136.7	1961.9	
		40	1092.8	882.3	1974.3	
		50	1351.1	661.6	2012.5	
An 3	50	20	561.4	1653.2	2212.7	2147.4
		30	865.8	1329.0	2194.9	
		40	1203.5	1005.4	2205.9	
		50	1459.8	735.3	2193.3	
C 6	100	20	68.4	421.0	489.2	492.3
		30	133.2	356.4	489.7	
		40	205.7	287.8	493.4	
		50	275.7	214.7	490.3	
C 12	50	30	30.9	102.3	133.1	136.7
		40	49.2	86.2	135.4	
		50	70.2	66.0	136.1	
		60	88.3	46.1	134.3	
T 2	50	30	795.2	1337.0	2128.9	2148.9
		40	1004.9	1138.7	2143.5	
		50	1241.8	879.4	2120.2	
		60	1515.2	661.6	2176.4	
T 19	50	30	1004.3	1793.3	2796.9	2783.1
		40	1286.4	1489.5	2775.6	
		50	1567.5	1225.9	2793.4	
		60	1888.3	932.0	2820.3	
Bu 5	80	10	34.1	47.0	81.1	78.8
		20	45.4	34.5	79.8	
		30	55.1	26.8	80.6	
		40	62.4	17.5	78.9	
Bu 8	80	10	21.7	38.6	59.8	59.9
		20	34.7	26.6	60.7	
		30	39.8	20.9	59.9	
		40	42.6	16.4	58.9	
S 50	100	10	70.7	170.6	241.2	246.4
		15	106.1	145.7	251.5	
		20	139.3	106.8	246.0	
		30	168.0	77.7	245.7	
456 A	100	25	39.1	92.7	131.7	132.7
		35	63.3	66.6	129.9	
		45	86.9	41.9	128.8	
		50	97.4	33.5	130.8	
456 B	100	20	5.1	19.2	24.3	24.0
		30	9.4	14.9	24.2	
		40	13.6	10.2	23.8	
		50	17.7	6.7	24.3	
578 A	100	25	46.3	139.8	186.1	185.0
		35	79.1	105.5	184.6	
		45	114.7	71.1	185.7	
		50	130.4	56.9	187.3	
578 B	80	20	4.9	24.3	29.2	29.5
		30	9.7	19.5	29.2	
		40	15.2	13.9	29.1	
		50	20.4	9.0	29.3	
P 6	50	20	131.5	308.9	438.5	437.9
		30	258.1	195.5	451.1	
		40	324.0	116.5	438.1	
		50	359.5	82.2	431.4	
P 7	50	20	98.3	327.0	423.3	433.0
		30	215.8	206.8	422.3	
		40	282.2	140.6	422.4	
		50	345.4	88.5	430.3	
P 8	50	30	70.2	279.7	349.9	352.8
		40	133.6	225.0	358.6	
		50	192.6	162.4	355.0	
		60	238.0	107.2	344.8	
Na 2	100	15	145.9	591.3	737.2	735.5
		20	206.9	527.5	734.3	
		30	353.1	376.2	729.3	
		40	492.9	244.4	736.8	
Km 3	50	30	368.1	1309.6	1676.7	1682.0
		40	516.5	1133.4	1648.9	
		50	745.7	950.3	1696.0	
		60	1011.0	673.1	1682.4	

[a] H is the steady field. During pARM acquisition the steady field was on from 100 mT AF to for $pARM_2$ and on from $\widetilde{H}$ to 0 mT for $pARM_1$. Σ pARM is the sum $pARM_1$ + $pARM_2$.

to ensure that we could easily compare pARMs produced in two perpendicular directions in additivity experiments (see section 3.2). Anisotropy of ARM (AARM) was measured by producing ARMs in six successive directions ($\pm z$, $\pm x$, $\pm y$) to obtain the AARM tensor. The three principal components (diagonal terms in AARM tensor) were required to be equal to within 3% and the six off-diagonal values smaller than 5% of the average principal component.

[17] The second criterion is unduly stringent for practical paleointensity work. *Selkin et al.* [2000] provide a method of correcting paleointensity values for moderate degrees of fabric anisotropy using the measured AARM tensor. We did not wish to apply any corrections in our experiments and as a result rejected a large fraction of out initial set of several hundred rock samples, although they passed the first selection criterion.

3.2. Additivity Tests

[18] Four synthetic and almost seven hundred natural samples were tested and rejected. For example, seventeen 0 age, ten 190 ka, and eight 380 ka oceanic basalts were prepared. Among these 35 samples from the East Pacific Rise, only three 380 ka Phoenix dredged basalts, P 6–8, passed sample selection criteria.

[19] Three different types of additivity experiment were carried out. In each case, the sum of partial ARMs was compared with the intensity of total ARM produced by a steady field H applied over the AF range 0–100 mT. In each type of experiment, we summed neighboring pARMs, i.e., pARMs in which H was applied over nonoverlapping intervals of AF that collectively covered the entire range 0–100 mT.

[20] In experiments of the first type, we produced conjugate pairs of pARMs with H applied over complementary parts of the 0–100 mT AF range. To generate $pARM_1$ ($\widetilde{H}_i$, 0 mT), no steady field H was applied while the AF was decaying from 100 mT to an intermediate level $\widetilde{H}_i$; H was applied only between $\widetilde{H}_i$ and 0. For $pARM_2$ (100 mT, $\widetilde{H}_i$), H was applied only over the AF range 100 mT to $\widetilde{H}_i$, and the added field was zeroed between $\widetilde{H}_i$ and 0. The process is shown schematically in Figure 4a. Four different conjugate pairs $pARM_1$ and $pARM_2$ were produced, using intermediate AF levels $\widetilde{H}_i$ sufficient to erase approximately 25%, 40%, 60% and 75% of the total ARM. For synthetic sample 1, for example, we used intermediate AF levels $\widetilde{H}_i$ = 20, 30, 40 and 50 mT.

[21] In experiments of the second type, we compared total ARM intensity with the sum of five neighboring pARMs (labeled $pARM_a$, $pARM_b$,., $pARM_e$). The AF intervals over which H was applied are nonoverlapping

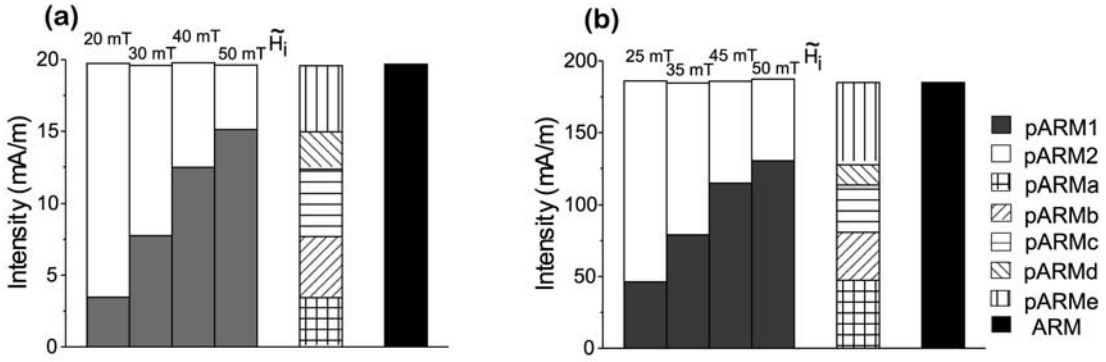

Figure 5. Additivity of pARMs for (a) sample 1 (0.065 μm) and (b) lake sediment sample 578 A.

and collectively cover the 0–100 mT range. The process is sketched in Figure 4b. The four intermediate AF levels at which H was switched on or off were the $\widetilde{H}_i$ same levels used to produce the four separate pairs ($pARM_1$, $pARM_2$) in the first experiment.

[22] Experiments of the third type also produced four conjugate pairs of partial ARMs, but the field H was rotated 90° between the ($\widetilde{H}_i$, 0) and (100 mT, $\widetilde{H}_i$) experiments. Thus $pARM_1$ was perpendicular rather than parallel to $pARM_2$. The purpose of producing orthogonal pARMs was to simulate remagnetization in nature, where secondary overprints may be at a large angle to pre-existing NRM. In the orthogonal experiment, the two pARMs were summed as scalar components rather than vectorially added.

[23] Before producing a new pARM, samples were AF demagnetized to 100 mT. Undemagnetized residuals were subtracted in calculating the pARM. Most experiments used a steady field $H = 50$ μT, but for weakly magnetic samples, 80 or 100 μT fields were used to amplify the signal.

4. Results

[24] Results of additivity tests for conjugate pairs of parallel pARMs appear in Tables 4 and 5. Typical examples (synthetic magnetite 1, mean size 0.065 μm; lake sediment 578 A) are plotted in Figures 5a and 5b. There are two main results. First, the sum of conjugate pairs of pARMs is equal to the total ARM within experimental error: $pARM_1 + pARM_2 = ARM$. The equality holds to within ±3% for all runs with all samples, and usually to better than ±1.5%. Second, there is no systematic bias. The sum of pARMs may be larger or smaller than the total ARM with about equal probability.

[25] Additivity results for sums of five adjacent parallel pARMs are given in Tables 6 and 7, with two typical examples plotted in Figures 5a and 5b. The sum of pARMs is again equal to total ARM within experimental error: $pARM_a + pARM_b + pARM_c + pARM_d + pARM_e = ARM$. Usually the equality holds to 1% or better; there are only two instances of 2.5–3% deviation. The sum of pARMs may again be larger or smaller than the total ARM, with a slight tendency to be smaller.

[26] A typical set of results of additivity experiments with pairs of orthogonal pARMs (for Cordova Gabbro C 12) is shown in Figure 6 and compared with the results for pairs of parallel pARMs for the same sample. The results of the perpendicular and parallel experiments are indistinguishable. Not only does the law of additivity of partial ARMs hold when the pARMs are orthogonal, the individual pARMs have exactly the same magnitudes. Thus there is no memory of prior pARM production in a different direction when full AF demagnetization is carried out between experiments. (In companion paper 2, we shall examine the details of how each pARM demagnetizes at different AF levels.)

5. Discussion

[27] The law of additivity of partial ARMs was verified at a high level of confidence in our experiments, with a universality that was unanticipated. For every sample tested, most containing magnetite but some (P 6–8, Km 3) with Ti-rich titanomagnetites, the sum of partial ARMs partitioning the 0–100 mT AF range exactly equaled the intensity of total ARM produced over the same range. This was true whatever the domain state of the magnetic carriers. It was true whether the total AF range was divided into two or five intervals for pARM production. Compounding of experimental errors might have been expected with the finer subdivision, but this was not evident in the results. Additivity was also independent of whether the intermediate field(s) $\widetilde{H}_i$ lay within the soft, intermediate, or hard part of the coercivity spectrum.

[28] These observations are rather astonishing because the analogous law of additivity of partial TRMs is increasingly

Table 6. Experimental Results for Additivity of Five Adjacent pARMs for Synthetic Samples[a]

Sample	$pARM_a$, mA/m	$pARM_b$, mA/m	$pARM_c$, mA/m	$pARM_d$, mA/m	$pARM_e$, mA/m	$\sum$ pARM, mA/m	ARM, mA/m
1	3.43	4.26	4.67	2.60	4.61	19.56	19.68
2	3.88	5.08	5.31	3.10	3.60	20.92	20.88
3	4.63	5.62	5.17	4.46	7.36	27.66	27.53
4	7.11	9.25	7.30	4.97	6.53	35.16	35.26
5	1.88	1.79	1.76	1.76	3.15	10.33	10.30
6	3.13	3.08	3.14	2.21	4.38	15.94	16.05
7	1.10	1.85	2.15	1.45	1.56	8.06	8.27
8	0.88	1.42	2.59	1.36	1.95	8.19	8.27
9	8.30	17.56	24.49	13.64	25.48	89.43	89.11
10	18.80	30.81	30.75	19.64	37.64	137.59	137.79

[a] Σ pARM is the sum $pARM_a + pARM_b + pARM_c + pARM_d + pARM_e$.

Table 7. Experimental Results for Additivity of Five Adjacent pARMs for Natural Samples[a]

Sample	H, μT	$pARM_a$, mA/m	$pARM_b$, mA/m	$pARM_c$, mA/m	$pARM_d$, mA/m	$pARM_e$, mA/m	$\sum$ pARM, mA/m	ARM, mA/m
An 1	50	549.0	270.6	253.6	241.3	670.8	1982.8	1960.1
An 3	50	565.4	293.6	322.9	245.0	731.9	2155.0	2147.4
C 6	100	67.8	63.3	70.3	71.4	215.3	487.2	492.3
C 12	50	30.7	18.0	19.6	18.5	46.2	133.0	136.7
T 2	50	797.6	206.7	236.1	265.2	664.4	2166.7	2148.9
T 19	50	1000.0	271.5	282.6	311.9	922.4	2787.8	2783.1
Bu 5	80	32.9	13.1	8.8	8.5	18.3	79.4	78.8
Bu 8	80	21.8	12.5	6.3	2.7	16.7	59.2	59.9
S 50	100	68.4	33.7	30.5	31.4	77.8	241.3	246.4
456 A	100	39.3	24.9	22.8	9.8	34.5	131.2	132.7
456 B	100	5.1	4.3	4.3	3.9	6.6	24.3	24.0
578 A	100	47.4	33.5	32.6	14.1	57.4	184.8	185.0
578 B	80	4.9	4.4	5.4	5.0	8.9	28.6	29.5
P 6	50	127.5	128.0	71.3	37.6	78.4	438.3	437.9
P 7	50	100.9	114.8	64.7	65.6	83.8	428.1	433.0
P 8	50	70.1	64.1	62.0	47.2	111.7	348.1	352.8
Na 2	100	144.7	59.4	143.9	140.2	248.7	734.3	735.5
Km 3	50	364.2	148.8	231.9	242.8	667.8	1654.4	1682.0

[a] H is the steady field. Σ pARM is the sum of $pARM_a$ + $pARM_b$ + $pARM_c$ + $pARM_d$ + $pARM_e$.

compromised with increasing grain size, with increasing number of pTRMs summed, and in higher ranges of the blocking temperature spectrum. *Shcherbakova et al.* [2000], for example, reported violation of pTRM additivity for MD grains, but we found that additivity of pARMs holds just as well for coarse-grained synthetic magnetites and for clearly MD granites (Bu 5, Bu 8, S 50) as it does for SD and PSD size magnetites and titanomagnetites. Likewise, additivity of pTRMs holds best when the intermediate temperature at which H is switched on or off is relatively low [e.g., *McClelland and Sugiura*, 1987], but the sum of pARMs matches total ARM equally well for intermediate fields $\widetilde{H}_i$ throughout the coercivity spectrum (Tables 4 and 5).

[29] The sum of pARMs shows no systematic tendency to be larger (even slightly larger) than the total ARM, in contrast to the situation with pTRM additivity, where the sum of pTRMs is always somewhat larger than the total TRM intensity [*Ozima and Ozima*, 1965; *Dunlop and West*, 1969; *Levi*, 1979; *McClelland and Sugiura*, 1987]. The major part of this excess is due to high-temperature isothermal remanence (IRM), which comes about because of the dwell time necessary to achieve a stable temperature before turning H on or off. IRM production is most noticeable at temperatures within ≈100°C of the Curie point, explaining why lower-T pTRMs add better. Also the more pTRMs are used, the more IRMs are included in the sum and the greater the overshoot compared to total TRM intensity. Because partial ARMs are produced at room temperature over brief times, IRM acquisition is minimal. This is probably the reason for the universally close match between pARM sums and total ARM.

[30] Grain interactions must be significant in the synthetic and even in many of the natural samples. Interactions are known to have a considerable effect on ARM and TRM intensities [*Jaep*, 1971; *Dunlop et al.*, 1975; *Sugiura*, 1979]. According to *Sugiura* [1979], the effect of interactions on ARM is detectable even for magnetite volume fractions as low as 0.01%. In spite of this, the additivity law was experimentally satisfied for all samples, regardless of magnetite concentration, implying that interactions affect partial and total ARM intensities in identical ways.

[31] The fact that pARMs are additive for high-Ti titanomagnetites (P 6–8, Km 3, Tables 5 and 7), which are typical NRM carriers in oceanic basalts and other rapidly cooled volcanic rocks, suggests that ARM methods of paleointensity determination could be suitable for these rocks. Titanium-rich titanomagnetites/titanomaghemites are usually unsuitable for Thellier-type paleointensity determination because they alter to multiphase assemblages with only mild heating.

6. Conclusions

1. The law of additivity of partial ARMs has been verified for all synthetic and natural samples to within ±3% (in more than half the samples, to better than ±1%). The universal validity of pARM additivity, for MD as well as SD and PSD magnetites, is in contrast to pTRM additivity, which is increasingly violated for larger MD grain sizes.

2. Additivity holds equally well whether the pARMs split the total AF range at a low coercivity, split the range at a high coercivity, or divide the range into five intervals spaced more or less evenly across the coercivity spectrum. This is in contrast to pTRM additivity, which tends to be violated for high-temperature pTRMs or multiple pTRMs because of the production of isothermal remanence.

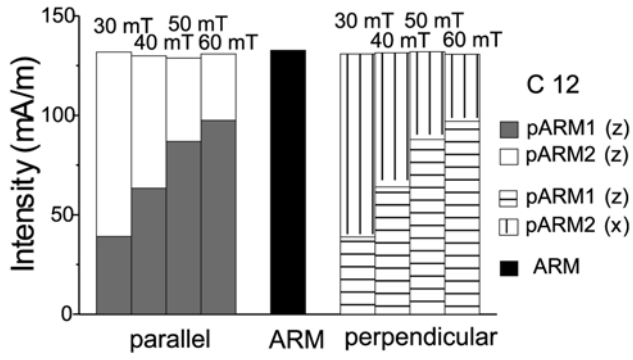

Figure 6. Additivity test for orthogonal pARMs (Cordova Gabbro sample C 12).

3. The explanation of 1 and 2 is probably that pARM is produced at room temperature over brief time intervals, minimizing effects like domain nucleation, domain wall equilibration, and IRM production that compromise pTRM additivity in MD grains at high temperatures.

4. Grain interactions have no detectable effect on pARM additivity.

5. High-Ti titanomagnetites also obey the law of additivity of pARMs. Because they alter on heating, they are generally unsuitable for Thellier paleointensity determination but may respond better to pseudo-Thellier or other ARM-related paleointensity techniques.

[32] **Acknowledgments.** Stephanie Brachfeld and Jeff Gee generously donated large collections of lake sediment and oceanic basalt samples for use in this study. John King, Lisa Tauxe, and Jean-Pierre Valet provided helpful reviews and suggestions. Fred Neub of the Materials Engineering Dept., University of Toronto helped with the SEM work. This research has been supported by the Natural Sciences and Engineering Research Council of Canada through grant A7709 to D.J.D.

References

Bagina, O. L., and G. N. Petrova, Determination of paleomagnetic field intensity using anhysteretic remanent magnetization, *Phys. Earth Planet. Inter.*, *13*, 363–367, 1977.

Bailey, M. E., and D. J. Dunlop, On the use of anhysteretic remanent magnetization in paleointensity determination, *Phys. Earth Planet. Inter.*, *13*, 360–362, 1977.

Banerjee, S. K., and J. P. Mellema, A new method for the determination of paleointensity from the ARM properties of rocks, *Earth Planet. Sci. Lett.*, *23*, 177–184, 1974.

Batiza, R., Y. Niu, J. L. Karsten, W. Boger, E. Potts, L. Norby, and R. Butler, Steady and non-steady state magma chambers below the East Pacific Rise, *Geophys. Res. Lett.*, *23*, 221–224, 1996.

Brachfeld, S. A., and S. K. Banerjee, A new high-resolution geomagnetic relative paleointensity record for the North American Holocene: A comparison of sedimentary and absolute intensity data, *J. Geophys. Res.*, *105*, 821–834, 2000.

Coe, R. S., Paleointensities of the Earth's magnetic field determined from Tertiary and Quaternary rocks, *J. Geophys. Res.*, *72*, 3247–3262, 1967.

Day, R., M. Fuller, and V. A. Schmidt, Hysteresis properties of titanomagnetites: Grain-size and compositional dependence, *Phys. Earth Planet. Inter.*, *13*, 260–267, 1977.

Dunlop, D. J., The rock magnetism of fine particles, *Phys. Earth Planet. Inter.*, *26*, 1–26, 1981.

Dunlop, D. J., Paleomagnetism of Archean rocks from northwestern Ontario, 4, Burchell Lake granite, Wawa-Shebandowan Subprovince, *Can. J. Earth Sci.*, *21*, 1098–1104, 1984.

Dunlop, D. J., Theory and application of the Day plot (M_{rs}/M_s versus H_{cr}/H_c), 1, Theoretical curves and tests using titanomagnetite data, *J. Geophys. Res.*, *107*(B3), 2056, 10.1029/2001JB000486, 2002.

Dunlop, D. J., and K. S. Argyle, Thermoremanence, anhysteretic remanence and susceptibility of submicron magnetites: Nonlinear field dependence and variation with grain size, *J. Geophys. Res.*, *102*, 20,199–20,210, 1997.

Dunlop, D. J., and Ö. Özdemir, *Rock Magnetism: Fundamentals and Frontiers*, 573 pp., Cambridge Univ. Press, New York, 1997.

Dunlop, D. J., and G. F. West, An experimental evaluation of single domain theories, *Rev. Geophys.*, *7*, 709–757, 1969.

Dunlop, D. J., M. E. Bailey, and M. F. Westcott-Lewis, Lunar paleointensity determination using anhysteretic remanence (ARM): A critique, *Geochim. Cosmochim. Acta*, *39*, 3063–3069, 1975.

Dunlop, D. J., L. D. Schutts, and C. J. Hale, Paleomagnetism of Archean rocks from northwestern Ontario, 3, Rock magnetism of the Shelley Lake granite, Quetico Subprovince, *Can. J. Earth Sci.*, *21*, 879–886, 1984.

Gee, J., and D. V. Kent, Calibration of magnetic granulometric trends in oceanic basalts, *Earth Planet. Sci. Lett.*, *170*, 377–390, 1999.

Jackson, M., W. Gruber, J. Marvin, and S. K. Banerjee, Partial anhysteretic remanence and its anisotropy: Applications and grain-size-dependence, *Geophys. Res. Lett.*, *15*, 440–443, 1988.

Jackson, M., H.-W. Worm, and S. K. Banerjee, Fourier analysis of digital hysteresis data: Rock magnetic applications, *Phys. Earth Planet. Inter.*, *65*, 78–87, 1990.

Jaep, W. F., Role of interactions in magnetic tapes, *J. Appl. Phys.*, *42*, 2790–2794, 1971.

Kono, M., Reliability of paleointensity methods using alternating field demagnetization and anhysteretic remanence, *Geophys. J. R. Astron. Soc.*, *54*, 241–261, 1978.

Levi, S., The additivity of partial thermal remanent magnetization in magnetite, *Geophys. J. R. Astron. Soc.*, *59*, 205–218, 1979.

Levi, S., and R. T. Merrill, A comparison of ARM and TRM in magnetite, *Earth Planet. Sci. Lett.*, *32*, 171–184, 1976.

Levi, S., and R. T. Merrill, Properties of single-domain, pseudo-single-domain, and multidomain magnetite, *J. Geophys. Res.*, *83*, 309–323, 1978.

Markert, H., and F. Heller, Determination of paleointensities of the geomagnetic field from anhysteretic remanent magnetization, *Phys. Stat. Solid. A*, *14*, K47, 1972.

McClelland, E., and N. Sugiura, A kinematic model of TRM acquisition in multidomain magnetite, *Phys. Earth Planet. Inter.*, *46*, 9–23, 1987.

Özdemir, Ö., and S. K. Banerjee, A preliminary magnetic study of soil samples from west central Minnesota, *Earth Planet. Sci. Lett.*, *59*, 393–403, 1982.

Ozima, M., and M. Ozima, Origin of thermoremanent magnetization, *J. Geophys. Res.*, *70*, 1363–1369, 1965.

Patton, B. J., and J. L. Fitch, Anhysteretic remanent magnetization in small steady fields, *J. Geophys. Res.*, *67*, 307–311, 1962.

Rimbert, F., Contribution à l'étude de l'action de champs alternatifs sur les aimantations rémanentes des roches, Applications géophysiques, *Rev. Inst. Fr. Pét.*, *14*(17–54), 123–155, 1959.

Rolph, T. C., and J. Shaw, A new method of paleofield magnitude correction for thermally altered samples and its application to lower Carboniferous lavas, *Geophys. J. Int.*, *80*, 773–781, 1985.

Selkin, P. A., J. S. Gee, L. Tauxe, W. P. Meurer, and A. Newell, The effect of remanence anisotropy on paleointensity estimates: A case study from the Archean Stillwater Complex, *Earth Planet. Sci. Lett.*, *183*, 403–416, 2000.

Senanayake, W. E., M. W. McElhinny, and P. L. McFadden, Comparison between the Thellier's and Shaw's paleointensity methods using basalts less than 5 million years old, *J. Geomagn. Geoelectr.*, *34*, 141–161, 1982.

Shaw, J., A new method of determining the magnitude of the paleomagnetic field, *Geophys. J. R. Astron. Soc.*, *39*, 133–141, 1974.

Shcherbakova, V. V., V. P. Shcherbakov, and F. Heider, Properties of partial thermoremanent magnetization in pseudo-single-domain and multidomain magnetite grains, *J. Geophys. Res.*, *105*, 767–781, 2000.

Stephenson, A., and D. W. Collinson, Lunar magnetic field paleointensities determined by an anhysteretic remanent magnetization method, *Earth Planet. Sci. Lett.*, *23*, 220–228, 1974.

Sugiura, N., ARM, TRM and magnetic interactions: concentration dependence, *Earth Planet. Sci. Lett.*, *46*, 438–442, 1979.

Tauxe, L., Sedimentary records of relative paleointensity of the geomagnetic field: Theory and practice, *Rev. Geophys.*, *31*, 319–354, 1993.

Tauxe, L., T. Pick, and Y. S. Kok, Relative paleointensity in sediments: A pseudo-Thellier approach, *Geophys. Res. Lett.*, *22*, 2885–2888, 1995.

Thellier, E., Sur l'aimantation des terres cuites et ses applications géophysiques, *Ann. Inst. Phys. Globe Univ. Paris Bur.*, *16*, 157–302, 1938.

Thellier, E., and O. Thellier, Sur l'intensité du champ magnétique terrestre dans le passé historique et géologique, *Ann. Geophys.*, *15*, 285–376, 1959.

Tsunakawa, H., and J. Shaw, The Shaw method of paleointensity determinations and its application to recent volcanic rocks, *Geophys. J. Int.*, *118*, 781–787, 1994.

Valet, J.-P., and E. Herrero-Bervera, Paleointensity experiments using alternating field demagnetization, *Earth Planet. Sci. Lett.*, *177*, 43–58, 2000.

Van Zijl, J. S. V., K. W. T. Graham, and A. L. Hales, The paleomagnetism of the Stormberg lavas of South Africa, 2, The behavior of the magnetic field during a reversal, *Geophys. J. R. Astron. Soc.*, *7*, 169–182, 1962.

Yu, Y., Rock magnetic and paleomagnetic experiments on hemoilmenites and titanomagnetites in some volcanic rocks from Japan, M. Sc. thesis, 24 pp., Univ. of Toronto, Toronto, Ont., 1998.

Yu, Y., and D. J. Dunlop, Paleointensity determination on the Tudor Gabbro, southern Ontario, *J. Geophys. Res.*, *106*, 26,331–36,343, 2001a.

Yu, Y., and D. J. Dunlop, Multivectorial paleointensity determination from the Cordova Gabbro, southern Ontario, *Earth Planet. Sci. Lett.*, in press, 2002.

Yu, Y., D. J. Dunlop, and Ö. Özdemir, Properties of partial anhysteretic remanent magnetization in magnetite, 2, Reciprocity, *J. Geophys. Res.*, *107*, doi:10.1029/2001JB001269, in press, 2002.

D. J. Dunlop, Ö. Özdemir, and Y. Yu, Room 3004, South Building, Geophysics, Department of Physics, University of Toronto at Mississauga, 3359 Mississauga Road North, Mississauga, Ontario, Canada L5L 1C6. (dunlop@physics.utoronto.ca; ozdemir@physics.utoronto.ca; yjyu@physics.utoronto.ca)